CHEMISTRY
A EUROPEAN JOURNAL

DOI: 10.1002/chem.200501370

Use of Dipicolinate-Based Complexes for Producing Ion-Imprinted Polystyrene Resins for the Extraction of Yttrium-90 and Heavy Lanthanide Cations

Anne-Sophie Chauvin,[a] Jean-Claude G. Bünzli,[a] François Bochud,[b] Rosario Scopelliti,[a] and Pascal Froidevaux*[b]

Abstract: Highly selective separation of yttrium (and lanthanides) is of interest for the design of radiopharmaceuticals, and an efficient method based on the ion-imprinting concept is proposed here. The synthesis and structural, thermodynamic and photophysical characterization of complexes of trivalent yttrium and lanthanides with two new vinyl derivatives of dipicolinic acid, **HL1** and **L2**, are described. The feasibility of using ion-imprinted resins for yttrium and lanthanide separation is demonstrated. The resins were obtained by copolymerization with styrene and divinylbenzene and subsequent acid treatment to remove the metal ion. High-resolution Eu luminescence experiments revealed that the geometry of the complexation sites is well preserved in the imprinted polymers. The ion-imprinted polymer based on **HL1** proved to be particularly well adapted for yttrium extraction, having a sizeable capacity (8.9 ± 0.2 mg g^{-1} resin) and a fast rate of extraction ($t_{1/2} = 1.7$ min). In addition, lighter and heavier lanthanide ions are separated. Finally, the resin displays high selectivity for yttrium and lanthanide cations against alkali and alkaline earth metals. For instance, in a typical experiment, 10 mg of yttrium was extracted from 5 g of milk ash sample by 2 g of the resin. The good separation properties displayed by the resin based on **HL1** open interesting perspectives for the production of highly pure ^{90}Y and radiolanthanides for medical applications, and for trace analysis of these radiochemicals in food and in the environment.

Keywords: copolymerization · extraction · lanthanides · polymers · yttrium

Introduction

Extraction and separation of metal cations have always been challenging analytical problems. Among the methods used, solid-phase extraction (SPE) is one of the most popular and efficient techniques. It merges the easy handling of a chromatographic method with the efficiency of solvent extraction. Recently, the preparation of new materials for metal-cation extraction based on the ion-imprinting concept was described: a matrix is synthesized in the presence of an ionic template and chelating resins are then obtained by removal of the targeted cation.[1–5] The cavities thus obtained in the polymer exhibit high selectivity towards specific metal ions, high capacity and the ability to deal with high concentrations of metal ions. Molecularly imprinted polymers have been successfully used as mimics of antibodies in an immunoassay-like technique[6,7] and of the active site of natural enzymes,[8–10] as well as in biorecognition.[11] Moreover, D'Souza et al. have shown that synthetic polymers can be imprinted with motifs of crystal surfaces so as to template the growth of specific crystal phases.[12] The preparation of styrene-based ion-imprinted resins initially involves formation of a vinyl monomer host in the presence of a bound guest acting as template. This vinyl monomer–template host–guest complex is then polymerized with a cross-linking agent, which provides spatially regulated sites in the polymer matrix. Numerous studies describing such methodologies were carried out in order to separate transition

[a] Dr. A.-S. Chauvin, Prof. Dr. J.-C. G. Bünzli, Dr. R. Scopelliti
Laboratory of Lanthanide Supramolecular Chemistry
École polytechnique fédérale de Lausanne
BCH 1402, 1015 Lausanne (Switzerland)

[b] Prof. Dr. F. Bochud, Dr. P. Froidevaux
Institute of Applied Radiophysics
University of Lausanne, Grand Pré 1
1007 Lausanne (Switzerland)
Fax: (+41) 21-623-3435
E-mail: Pascal.Froidevaux@chuv.ch

Supporting information for this article is available on the WWW under http://www.chemeurj.org/ or from the author.

metal cations, but few have dealt with lanthanides or actinides, and none specifically with the yttrium cation.[13–18]

Highly selective separation of yttrium and lanthanides is of interest for the design of radiopharmaceuticals for the treatment of illnesses such as cancer and rheumatism, and in the past decades there has been significant interest in yttrium detection in biological applications.[19,20] Presently, ^{89}Sr, ^{186}Re, ^{153}Sm, ^{166}Ho, ^{169}Er, ^{177}Lu and ^{90}Y radioisotopes are routinely used in clinical treatments,[21–23] and several ^{90}Y-labelled biomolecules have been tested for their therapeutic efficacy in tumour radiotherapy.[24] Moreover, ^{90}Sr, ^{90}Y, radiolanthanides and actinides are gaining growing interest in radio-ecological analyses and are taken into account when assessing public exposure to ionizing radiation. Specific needs for analytical procedures for these radioelements led to the development of classical exchange and extraction resins.[25–28] However, all these techniques suffer either from low specificity, as in cation- or anion-exchange chromatography, or, in the case of the Eichrom *Sr.spec* extraction-chromatography method for ^{90}Sr determination, of low tolerance to the calcium content of the matrix.[23] In addition, extraction-chromatography columns are processed by physical adsorption of the extracting molecule on a inert polymer support, which is not satisfactory for use in radiopharmaceutical applications, because the extracting molecule can diffuse into the radionuclide solution used for radiolabelling.

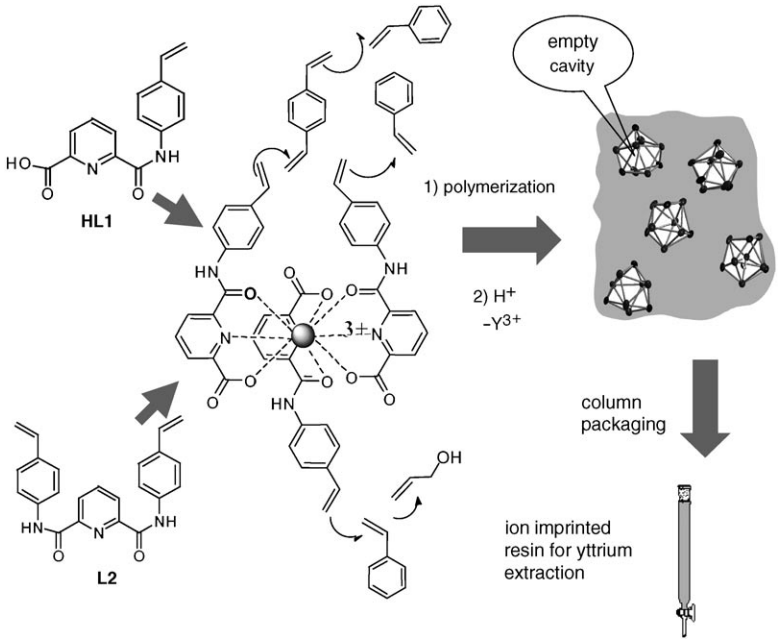

Figure 1. Schematic representation of the preparation of the imprinted polystyrene ion-exchange resin.

The aim of this work was the development of a new extraction resin with high specificity for yttrium and lanthanides. The possibility of analyzing ^{90}Sr in numerous environmental and biological samples by determining its daughter product ^{90}Y was recently demonstrated. The method involves complexation of trivalent yttrium by three dipicolinate ligands to give an anionic species that is subsequently extracted on a polystyrene-based anion exchanger.[29,30] Thus, we speculated that anchoring dipicolinate ligands on a styrene matrix in an appropriate geometry would produce a polymer suitable for the specific recognition and extraction of yttrium. Consequently, the ion-imprinting technique was used to impress trivalent yttrium cations in a cavity formed by three dipicolinate entities bearing a vinyl function (Figure 1). We describe the synthesis of two novel vinyl derivatives of dipicolinic acid, **HL1** and **L2**, their interaction with yttrium and lanthanide cations in solution and the solid-state properties of the isolated complexes. The last-named were used as templates for producing ion-imprinted resins that were tested for the separation of yttrium from high-calcium samples.

Results and Discussion

Synthesis and characterization of ligands HL1 and L2: Ligands **HL1** and **L2** were obtained from pyridine-2,6-dicarboxylic acid diethyl (**1**) and dimethyl ester (**2**), respectively (Scheme 1), synthesized from dipicolinic acid (dpa).[31] Vinylphenylamine was deprotonated in THF by addition of butyllithium and added to the esters, similarly to the procedure used for the addition of the lithium salt of diethylamine to ester **2**.[32] In both cases, addition of the lithium salt of vinylphenylamine led to the mono- or disubstituted compound as the major product, depending on the number of equivalents added. Equimolar mixtures of vinylphenylamine and pyridine-2,6-dicarboxylic acid ester gave both the mono- and disubstituted products with the methyl ester in ratio 60:40, while the monosubstituted product **3** was the major product with the diethyl ester (92:8). Therefore, dimethyl ester **2** was preferentially used for the preparation of **L2** and diethyl ester **1** for the synthesis of the monosubstituted precursor **3**. To obtain **HL1** in good yield, hydrolysis of **3** had to be performed under mild conditions; otherwise, the carboxamide moiety was also hydrolyzed upon heating and dpa was recovered.

In summary, **HL1** was obtained by a three-step procedure in 65% yield based on dpa, while **L2** was isolated in two steps with 75% yield. In [D_6]DMSO, both **HL1** and **L1**$^-$ display the expected eight signals arising from the aromatic and allylic protons, as well as a broad signal for the amide

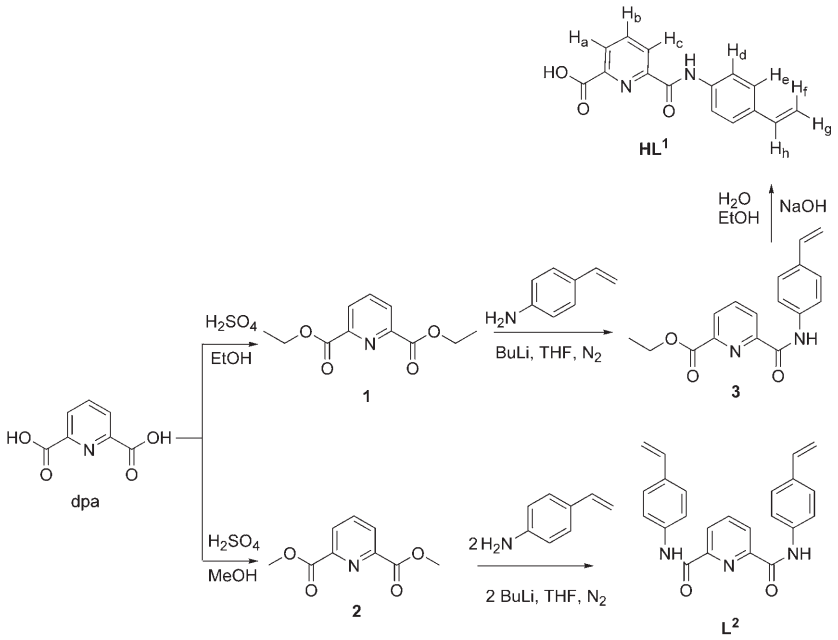

Scheme 1. Synthesis of **HL1** and **L2**.

proton (Table 1). In CD_3CN, **L2** presents seven signals, consistent with the presence of a C_2 symmetry axis.

Single crystals of **HL1** suitable for X-ray analysis were grown from methanol and their structure elucidated (Figure 2). The crystal arrangement shows a network of very strong OH···O hydrogen bonds (O2···O3, 2.657(2) Å, O2–H2···O3 175.3°) between neighbouring molecules with formation of infinite chains along the *b* axis. These chains are held together by weak N–H···O and CH···O interactions (for contact distances and angles, see Supporting Information). All bond lengths in **HL1** are standard and the ligand is nonplanar, as testified by the torsion angles N1-C1-C7-O3 (−161.5(2)°) and C7-N2-C8-C9 (−144.4(2)°), which indicate the relative position of the two aromatic rings. The presence of steric hindrance between O3 and H13 and H2A and H9 is revealed by the angles calculated between the following planes: (N1, C1–C5) and (C7, O3, N2) 19.8°, (N1, C1–C5) and (C8–C13) 35.5°, (C8–C13) and (C7, O3, N2) 54.6°.

Acidity constants of **HL1** were determined by spectrophotometric titration in H_2O/MeOH (99.5/0.5), by monitoring the spectral changes in the range 225–500 nm, from $(\mathbf{H_2L1})^+$ at pH 2.0 (precipitation occurs at pH < 2.0) up to pH 12. Fitting the data to deprotonation Equilibria (1) and (2) yielded $pK_{a1} = 2.8 \pm 0.4$ and $pK_{a2} = 3.9 \pm 0.4$.

$$(\mathbf{H_2L1})^+ \rightleftharpoons \mathbf{HL1} + H^+ \qquad K_{a1} \qquad (1)$$

$$\mathbf{HL1} \rightleftharpoons (\mathbf{L1})^- + H^+ \qquad K_{a2} \qquad (2)$$

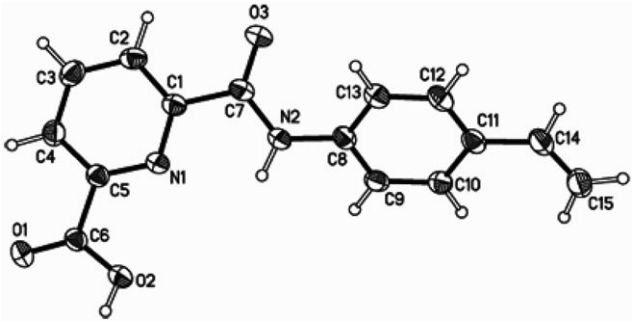

Figure 2. ORTEP view of the crystal structure of **HL1** showing the atom-numbering scheme; ellipsoids are represented at 50% probability.

The first value corresponds to deprotonation of the carboxylic acid, and the second to deprotonation of the pyridinium nitrogen atom. Compared with dipicolinic acid ($pK_a =$

Table 1. Chemical shifts [ppm] and coupling constants for **HL1**, Na**L1**, $[Y(\mathbf{L1})_3]$ in $[D_6]$DMSO, and **L2**, $[Ln(\mathbf{L2})_3]^{3+}$ (Ln = La, Y) in CD_3CN, at room temperature; see Scheme 1 for the numbering scheme of the protons.

	H_a	H_b	H_c	H_d	H_e	H_f	H_g	H_h	HNCO
HL1	8.31 d	8.27 dd	8.38 d	7.81 d	7.52 d	6.71 dd 17.7+11 Hz	5.79 d	5.22 d 11 Hz	11.07
	7.6 Hz	7.3+7.6 Hz	7.3 Hz	8.5 Hz	8.5 Hz		17.7 Hz		br
Na**L1**[a]	8.32 d	8.39 dd	8.36 d	7.88 d	7.55 d	6.75 dd 17.6+11 Hz	5.83 d	5.26 d 11 Hz	11.04
	7.8 Hz	7.6+7.8 Hz	7.6 Hz	8.6 Hz	8.6 Hz		17.6 Hz		br
$[Y(\mathbf{L1})_3]$	8.38 8.5 Hz	8.30 6.6+8.5 Hz	8.40 6.9 Hz	7.93 8.6 Hz	7.56 8.6 Hz	6.73 17.7+10.7 Hz	5.80 17.7 Hz	5.23 10.7 Hz	11.25
									br
L2	8.46 d	8.23 t 7.8 Hz	–	7.91 d	7.55 d	5.81 dd	6.80 d	5.26 d	10.12
	7.8 Hz			8.7 Hz	5.6 Hz	17.6+10.9 Hz	17.6 Hz	10.9 Hz	br
$[Y(\mathbf{L2})_3]^{3+}$	8.68 br	8.68 br	–	7.30 d	7.25 d	5.75 dd	6.67 d	5.30 d	10.17
				8.6 Hz	8.6 Hz	17.6+11.0 Hz	17.6 Hz	11.0 Hz	br
$[La(\mathbf{L2})_3]^{3+}$	8.48 d	8.37 t 7.8 Hz	–	7.76 d	7.44 d	6.75 dd	5.79 d	5.27 d	10.07
	7.8 Hz			8.2 Hz	8.2 Hz	17.6+10.9 Hz	17.6 Hz	10.9 Hz	br

[a] **HL1** was deprotonated with 1 equiv of NaOD, dried and dissolved in $[D_6]$DMSO prior to measurement.

2.16 and 4.76,[33] or 2.03 and 4.49[34]) the vinylic substituent substantially increases the acidity of the pyridinium nitrogen atom, while a concomitant decrease in the acidity of the carboxyl group is observed. The calculated distribution curves are shown in Figure 3: in aqueous solution at pH 7.4, the ligand is totally deprotonated.

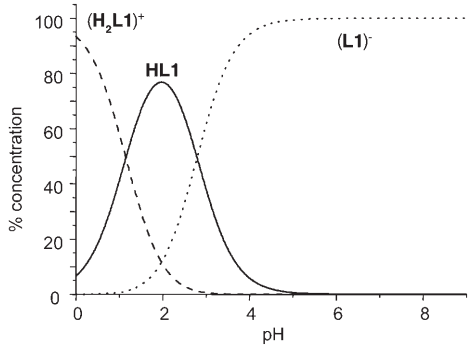

Figure 3. Distribution diagram for **HL1**, computed from the acidity constants given in the text.

Synthesis and characterization of the complexes: Complexes of **HL1** and **L2** with various lanthanides were synthesized either in methanol after deprotonation of **HL1** or in acetonitrile in the case of **L2**, by mixing the ligand and partially dehydrated $Ln(ClO_4)_3 \cdot n H_2O$ (Ln = Y, La, Eu, Gd, Tb; $n = 2.5$–4) in stoichiometric quantities. In all cases a yellow precipitate of the desired $[Ln(\mathbf{L1})_3] \cdot x H_2O$ and $[Eu(\mathbf{L2})_3](ClO_4)_3$ complexes was obtained in good yield (80–95%). The complexes with **L1** are soluble in DMSO and in water containing 0.5 vol% of methanol. Complexes with **L2** are hygroscopic; they are insoluble in water but they exhibit a solubility of 2×10^{-3} M in acetonitrile.

X-ray quality crystals of $[Eu(\mathbf{L2})_3](ClO_4)_3 \cdot 2 MeCN$ were grown by slow diffusion of *tert*-butyl methyl ether into a 10^{-3} M solution of the complex in acetonitrile. The compound crystallizes in the triclinic space group $P\bar{1}$ and features discrete $[Eu(\mathbf{L2})_3]^{3+}$ cations and uncoordinated perchlorate anions (Table 2, Figure 4). The crystal arrangement is characterized by rather strong hydrogen bonds between NH moieties, one acetonitrile molecule and the perchlorate anions (see Supporting Information). There are also weak interactions between most aromatic and allylic carbon atoms and perchlorate anions or the acetonitrile molecule not interacting with NH. Finally, weak interligand contacts take place through CH···π ring interactions but no direct π–π interaction is observed. In the $[Eu(\mathbf{L2})_3]^{3+}$ complex cation, the three ligand strands are analogously wrapped around the europium ion. The latter is nine-coordinate, with a slightly distorted tricapped trigonal prismatic coordination polyhedron close to D_3 symmetry, in which the six oxygen atoms occupy the vertices and the three nitrogen atoms of the pyridine rings lie on the capping positions, forming an equatorial plane. The metal ion is located symmetrically with respect to the two planes defining the bases of the prism P1 (O1A, O1B, O2C) and P2 (O1C, O2A, O2B), with Eu–P1 and Eu–P2 distances of 1.726 (5) and 1.697(5) Å, respectively. Moreover, the deviation of the Eu ion from the equatorial plane defined by (N1A, N1B, N1C) is only 0.072(6) Å. Finally, the two distal planes P1 and P2 are almost parallel, with an interplanar angle of 1.8(1)°. The average Eu–O bond length is 2.414(8), which is identical, within experimental error, to that of 2.410(13) Å reported in the literature for the tris complex with pyridine-2,6-dicarboxylic acid bis(diethylamide).[35] On the other hand, the mean Eu–N distance of 2.527(9) Å is somewhat shorter than that of 2.554(13) Å reported for the bis-amide complex.[35]

Table 2. Selected bond lengths [Å] and angles [°] in $[Eu(\mathbf{L2})_3](ClO_4)_3 \cdot 2 CH_3CN$.

	Ligand a	Ligand b	Ligand c
Eu–O1	2.415(8)	2.406(8)	2.402(6)
Eu–O2	2.417(7)	2.429(7)	2.417(8)
Eu–N1	2.522(8)	2.528(7)	2.530(8)
O1-Eu-N1	62.7(3)	63.2(3)	63.2(3)
N1-Eu-O2	63.6(3)	63.2(3)	68.8(3)
O1-Eu-O2	126.1(2)	126.3(2)	126.0(2)
N-Eu-N	119.0(2)[a]	118.6(2)[b]	122.2(3)[c]

[a] N1a-Eu-N1b. [b] N1b-Eu-N1c. [c] N1c-Eu-N1a.

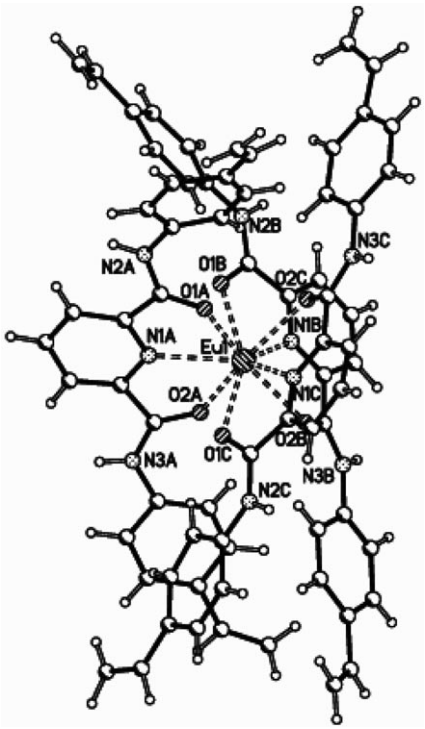

Figure 4. Ball-and-stick representation of $[Eu(\mathbf{L2})_3](ClO_4)_3$ with partial atom-numbering scheme.

The solution structure of the Y and La tris complexes was investigated by ^1H NMR spectroscopy (Table 1). In [D6]DMSO, distinct signals were observed for free and coordinated $\mathbf{L1}^-$, contrary to solutions of the complexes with **L2**, which only showed the signals of the free ligand. That is, the

strongly coordinating DMSO dissociates the complexes with **L2**, while the competition with $\mathbf{L1}^-$ is in favour of the latter. The stability of the complexes of $\mathbf{L1}^-$ in DMSO allows the use of this solvent in the polymerization of the complexes to increase their solubility. On the contrary, this solvent cannot be used when imprinting polymers with **L2** complexes.

The spectra of $[D_6]$DMSO (**L1**) and CD_3CN (**L2**) solutions containing a stoichiometric ratio Ln:L = 1:3 (Table 1) display the same number of signals as the free ligands, and this points to the equivalence, on the NMR timescale, of the three ligand strands and to an averaged trigonal arrangement of the complexes. The most shielded protons are those of the pyridine moiety, consistent with the fact that the pyridine nitrogen atom is coordinated to the metal ion. On the other hand, the presence of the metal ion has little effect on the allylic protons, which lie far from the coordination sphere. In conclusion, the presence of aromatic vinyl carboxamide derivatives substituting the 2- and/or 6-position of the pyridine moiety does not affect the formation of 1:3 Ln:L complexes, which exhibit a trigonal symmetry, as reported in the literature for other dipicolinic acid derivatives.[35–37]

The stability of the tris complexes was assessed by spectrophotometric titration of the ligands (1.4×10^{-4} M) with lanthanide perchlorates (10^{-3} M). The absorption spectra of the ligands display three main bands located around 45900, 38600 and 33000 cm^{-1} for $\mathbf{L1}^-$ in Tris-HCl buffer (0.1 M, pH 7.45), and 50700, 38460 and 33000 cm^{-1} for **L2** in acetonitrile. The more energetic bands are assigned to transitions mainly centred on the carbonyl groups and the middle band to $n\rightarrow\pi$ and $\pi\rightarrow\pi^*$ transitions located on the pyridine units, while the less energetic transitions contain substantial contributions from the vinyl substituent, according to calculations performed with the CAChe Pro 6.1 program package for Windows (Fujitsu Ltd., **2000–2003**). Upon complexation of $\mathbf{L1}^-$, the band at 33000 cm^{-1} undergoes a weak bathochromic shift of about 450 cm^{-1}, whereas the band at 38600 is blue-shifted (ca. 1100 cm^{-1}). In the complexes with **L2**, the band at 38460 is blue-shifted by about 1540 cm^{-1}, while that at 33300 cm^{-1} is red-shifted (ca. 2700–3000 cm^{-1}). The variation of the absorbance (see Supporting Information) was recorded versus $R_1=[Ln^{III}]_{tot}/[\mathbf{L1}^-]$ $(0<R_1<1.4)$ at pH 7.4, or $R_2=[Ln^{III}]_{tot}/[\mathbf{L2}]$ $(0<R_2<1.5)$. In each case, factor analysis pointed to the presence of three absorbing species, and data could be satisfactorily fitted to Equations (3)–(5). They are consistent with the successive formation of complexes with 1:1, 1:2, and 1:3 stoichiometries, and the corresponding $\lg\beta$ values are listed in Table 3

Table 3. Cumulative stability constants $\lg\beta_i$ for the complexes $[Ln(\mathbf{L1})_i]^{(3-i)+}$ $(i=1–3)$ in water buffered at pH 7.45 and $[Eu(\mathbf{L2})_i]^{3+}$ in acetonitrile at 25 °C; 2σ is given in parentheses.

Complex	$\lg\beta_1$	$\lg\beta_2$	$\lg\beta_3$
$[Eu(\mathbf{L1})_i]^{(+3-i)}$	7.9(6)	14.0(7)	19.9(7)
$[Tb(\mathbf{L1})_i]^{(+3-i)}$	7.8(5)	13.8(7)	19.7(7)
$[La(\mathbf{L2})_i]^{3+}$	7.9(2)	14.6(1)	19.8(3)
$[Eu(\mathbf{L2})_i]^{3+}$	8.1(2)	14.6(1)	19.3(2)
$[Tb(\mathbf{L2})_i]^{3+}$	8.0(1)	14.3(1)	19.7(3)
$[Y(\mathbf{L2})_i]^{3+}$	7.6(1)	14.2(1)	20.4(1)

$$Ln^{3+} + (\mathbf{Lx})^{i-} \rightleftarrows [Ln(\mathbf{Lx})]^{(3-i)+} \quad \lg\beta_1 \tag{3}$$

$$Ln^{3+} + 2\,(\mathbf{Lx})^{i-} \rightleftarrows [Ln(\mathbf{Lx})_2]^{(3-2i)+} \quad \lg\beta \tag{4}$$

$$Ln^{3+} + 3\,(\mathbf{Lx})^{i-} \rightleftarrows [Ln(\mathbf{Lx})_3]^{(3-3i)+} \quad \lg\beta_3 \tag{5}$$

where $x=1$, $i=1$ and $x=2$, $i=0$.

Since $\mathbf{L1}^-$ has one carboxylate group less than dpa^{2-}, the first two successive stability constants are about one order of magnitude smaller than those found by Grenthe[38] for dipicolinate complexes ($\Delta\lg K_1\approx0.7$, 0.8, and $\Delta\lg K_2\approx1.0$, 1.4 for Eu and Tb, respectively). On the other hand, the $\lg K_3$ values are similar for the two series of complexes ($\Delta\lg K_3\approx0.4$ and ≈0 for Eu and Tb, respectively), which can be explained by the smaller charge borne by $\mathbf{L1}^-$ being compensated by the fact that this ligand still interacts with a positively charged complex, while $[Ln(dpa)_2]^-$ is negatively charged.

The $\lg\beta_1$ and $\lg\beta_2$ values for the complexes with **L2** are identical, within experimental error, to those reported for the diethylamide-substituted ligand[35] but the $\lg\beta_3$ values are substantially smaller ($\Delta\lg\beta_3=1.2$, 3.0, 3.2, and 2.0 for La, Eu, Tb, and Y, respectively). This points to a minor electronic effect induced by the change in the amide substituents, while the substantial steric hindrance generated by the vinylbenzene group makes coordination of the third ligand more difficult.

Synthesis and characterization of polymers derived from $[Y(L1)_3]$ and $[Y(L2)_3](ClO_4)_3$: Imprinted polymers were produced from divinylbenzene, allyl alcohol and azobis(isobutyronitrile). The amount of $[Y(\mathbf{L1})_3]$ introduced into the polymer can reach 5 wt % if DMSO is added. For solubility reasons, imprinted polymers containing $[Y(\mathbf{L2})_3](ClO_4)_3$ could not be synthesized in the same way. Pyridine had to be added in all cases for better solubility of the complex and it also acted as a porogen, while allyl alcohol was added to increase the hydrophilicity of the polymer. After imprinting the polymer with $[Y(\mathbf{L1})_3]$ or $[Y(\mathbf{L2})_3](ClO_4)_3$, yttrium was extracted under acidic conditions to provide the corresponding metal-free yellow resins **R-Y-L1** and **R-Y-L2**, respectively. Three reference polymers were prepared: resin **R**, prepared from divinylbenzene and vinyl alcohol only, which does not contain any complex or ligand, and resins **R-L1** and **R-L2**, with uncoordinated **HL1** and **L2**, respectively. Furthermore a styrene polymer containing the highly luminescent tris(dipicolinate) complex $[Cs_3Eu(dpa)_3]$ (**R-Eu-dpa**) was synthesized to test the uniformity of distribution of the complex centres in the resin. Under UV/Vis light, the red colour due to the luminescence of the Eu complex showed the homogeneity of the polymer (Supporting Information). When the **R-Eu-dpa** resin is washed with 0.1 M HCl, the luminescence disappears, consistent with removal of the Eu^{III} cations.

The ion-imprinted polymer with $[Y(\mathbf{L1})_3]$ was analyzed with reflectance IR spectrometry. Its spectrum is compared in Figure 5 to those of polystyrene, free ligand, free complex

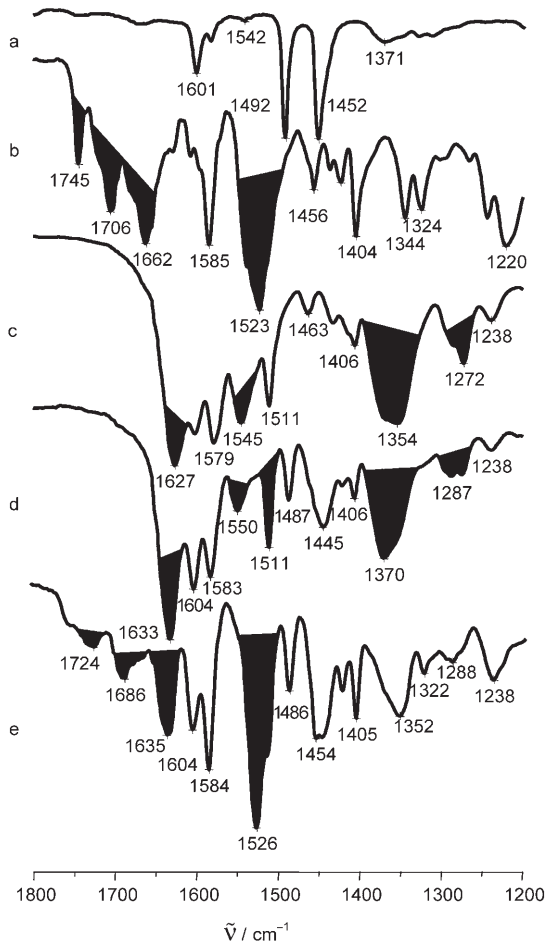

Figure 5. Part of the IR spectra of polystyrene (a), **L1** (b), [Y(**L1**)$_3$] (c), [Y(**L1**)$_3$] imprinted in the polymer (resin **R-Y-L1**, d) and metal-free resin **R-L1** after acid treatment (e).

[Y(**L1**)$_3$] and metal-free resin **R-Y-L1** (after acid treatment). The free ligand **HL1** displays three characteristic bands at 1662, 1706 and 1745 cm^{-1}, corresponding to vibrations of the pyridine double bonds and the carbonyl functions of the carboxyl and carboxamide groups (amide I), respectively. Upon coordination to yttrium in [Y(**L1**)$_3$], important shifts are expected for coordinated carboxylate:[39] the stretching frequencies are observed at 1545 cm^{-1} (ν_{as}) and 1370 cm^{-1} (ν_s). These values are close to those observed with dipicolinic acid, and $\Delta\tilde{\nu} = 175$ cm^{-1} points to monodentate coordination of the carboxylate.[40] One band appears at 1272 cm^{-1} which can be attributed to coordinated pyridine. In parallel, the intense band observed in **HL1** at 1523 cm^{-1}, mainly corresponding to the C–N=O stretching vibration, is shifted to 1511 cm^{-1}. Finally, one red-shifted and intense band at 1627 cm^{-1} is still observable, due to the pyridine double bonds. After polymerization of the complex, the resulting spectrum consists in a superposition of those of [Y(**L1**)$_3$] and polystyrene (cf. the bands at 1604, 1487, 1445 and 1370 cm^{-1} arising from the aromatic C–C bonds of styrene). The band at 1627 cm^{-1} is still observable, but slightly shifted to 1633 cm^{-1}, and this indicates that Y^{III} remains coordinated and that the complex was not destroyed upon polymerization. After acid treatment to provide metal-free resin **R-Y-L1**, the two carbonyl vibrations and that of the pyridine moiety are recovered, at 1724, 1686 and 1633 cm^{-1}, red-shifted by 20–30 cm^{-1} with respect to **HL1**. Additionally, the strong band at 1526 cm^{-1} is also recovered, so that the spectrum is close to a superposition of the spectra of polystyrene and the free ligand. To test the reversibility of complexation, resin **R-Y-L1** was charged with europium: an IR spectrum close to that of the resin containing the yttrium complex was obtained, that is, the metal is complexed in the imprinted **L1**$^-$-containing cavity.

Photophysical properties of the ligands and complexes: Photophysical data are presented in Table 4. On excitation of **L1**$^-$ (10^{-4} M in 0.1 M Tris-HCl buffer) at 36600 cm^{-1}, one emission band appeared, centred at 25600 cm^{-1}, with a shoulder around 23000 cm^{-1} (Figure 6), which fades at room temperature upon enforcement of a time delay. On the other hand, the band shifts to 24800 cm^{-1} at 77 K (with 10% glycerol added), and it can be resolved into two components, with maxima at 26300 and 24600 cm^{-1}, respectively, with relative integrated intensities of 40 and 60%. We assign the former as arising from a singlet state and the latter from a triplet state. Similar observations could be made for **L2** (2×10^{-4} M in acetonitrile), although in this case emission from both $^1\pi\pi^*$ (24950 cm^{-1}) and $^3\pi\pi^*$ (21900 cm^{-1}) states is detected at room temperature and at 77 K (24000 and 21500 cm^{-1} with relative intensities of 45 and 55%, respectively). The energy gap between the $^3\pi\pi^*$ and $^1\pi\pi^*$ states ($\Delta E = 1400$ cm^{-1} for **L1**$^-$ and 2000 cm^{-1} for **L2**) is quite small, but the intersystem-crossing yield, esti-

Table 4. Ligand-centred absorption and emission properties of **L2** and [Ln(**L2**)$_3$](ClO$_4$)$_3$ in CD$_3$CN, **L1**$^-$ and the [Ln(**L1**)$_3$] in water at pH 7.4, 5×10^{-4} M (Ln = La, Gd, Eu, Tb).

Compound	Absorption spectrum {E [cm^{-1}] (lgε)[a]}	E [cm^{-1}] $^1\pi\pi^*$[b]	E [cm^{-1}] $^3\pi\pi^*$[c]	τ [ms][d]
L1$^-$	33000 (4.1); 38460 (4.0); 45870 (4.0)	25 600	*24550*, 27000*	0.32(3)
[La(**L1**)$_3$]	32400(4.1); 39525 (4.2); 50600 (4.1)	25800	*23400*, 26200*	–
[Eu(**L1**)$_3$]	32400(4.1); 39200 (4.2); 50600 (4.1)	–	*23600*, 26400*	5.06(4)
[Gd(**L1**)$_3$]	32800 (4.1); 39100 (4.2); 50600 (4.1)	–	*23850*, 26500*	–
[Tb(**L1**)$_3$]	32600(4.1); 39150 (4.2); 50600 (4.1)	24200	*23 800*, 26200*	4.47(3)
L2	33000(4.5); 38500 (4.4); 50680 (4.9)	24500	22700, 26500*	0.25(3)
[La(**L2**)$_3$](ClO$_4$)$_3$	33230 (4.5); 38570 (4.4); 50300(4.9)	22300	*21100*, 24700*	-
[Eu(**L2**)$_3$](ClO$_4$)$_3$	32630 (4.4); 38950 (4.4); 50230(4.9)	–	*21500*, 24800*	4.75(3)
[Gd(**L2**)$_3$](ClO$_4$)$_3$	32780 (4.4); 38950(4.4); 50530(4.9)	22500	*21600*, 24600*	–
[Tb(**L2**)$_3$](ClO$_4$)$_3$	32550 (4.5); 38500 (4.3); 50680 (4.9)	22900	*21800*, 24400*	3.77(3)

[a] Maxima of the band envelopes at 295 K. [b] From fluorescence spectra at 295 K; energies are given for the maxima of the band envelopes (in italics), and 0-phonon transitions are marked with asterisks. [c] From phosphorescence spectra of frozen solutions at 77 K. [d] Lifetimes in frozen solutions at 77 K.

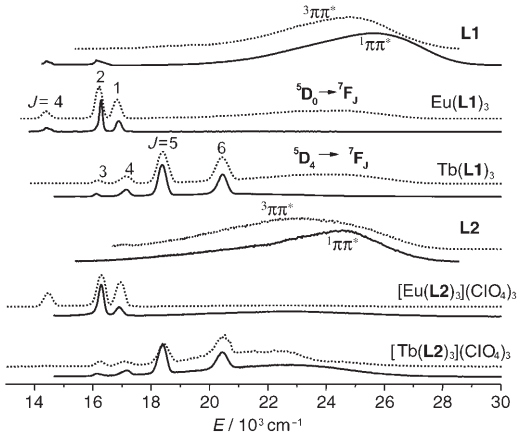

Figure 6. Luminescence spectra of **HL1** and **L2** and their complexes $[Ln(\mathbf{L1})_3]$ and $[Ln(\mathbf{L2})_3](ClO_4)_3$ (Ln = Eu, Tb), at 295 K (solid lines, without time delay) and 77 K (dotted lines, with a 0.05 ms time delay); solvents: MeCN for **L2** and its complexes (2×10^{-4} M), Tris-HCl 0.1 M, pH 7.45 for **L1** and its complexes (10^{-4} M); spectra recorded at 77 K were excited at 36 630 cm^{-1} and the solutions contained 10% glycerol.

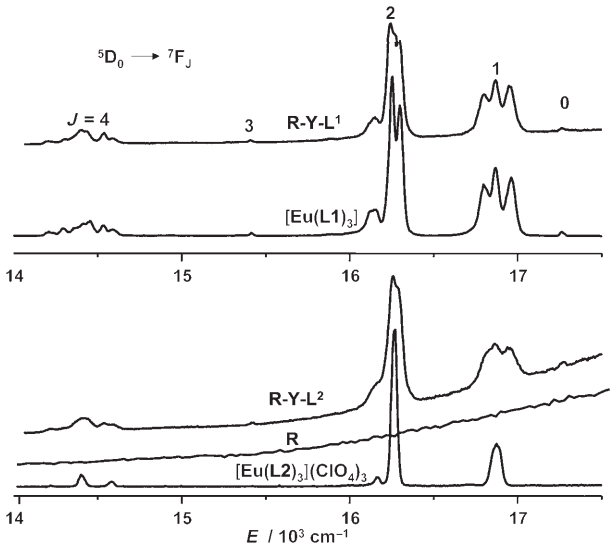

Figure 7. Luminescence spectra of $[Eu(\mathbf{L1})_3]$ and the corresponding imprinted resin (top), and $[Eu(\mathbf{L2})_3](ClO_4)_3$, the corresponding imprinted resin and the metal-free resin (bottom). Microcrystalline samples at 77 K with 0.01 ms time delay and excitation at 36 630 cm^{-1}.

mated from the relative area of the $^1\pi\pi^*$ and $^3\pi\pi^*$ emissions at 77 K, remains sizeable: 60% for $\mathbf{L1}^-$ and 55% for **L2**.

The lifetimes of the $^3\pi\pi^*$ states are short, but similar given the different solvents used (320 μs for $\mathbf{L1}^-$ and 250 μs for **L2**). After complexation with La^{III}, Gd^{III}, Eu^{III}, or Tb^{III}, these bands are slightly shifted (see Table 4). In addition, the Eu^{III} and Tb^{III} complexes display the characteristic narrow emission lines of the metal ions that reflect $^3\pi\pi^*\rightarrow$ Ln energy transfer. This is more efficient with Eu^{III}, since no triplet phosphorescence was observed with this ion, although some singlet-state emission was still detected. The luminescence decays at 77 K are single exponential functions and their analysis leads to $^5D_0$(Eu) lifetimes of 5.06 ± 0.04 and 4.75 ± 0.03 ms for complexes with $\mathbf{L1}^-$ and **L2**, respectively, and to $^5D_4$(Tb) lifetimes of 4.47 ± 0.03 and 3.77 ± 0.03 ms, which reflect absence of interaction with OH oscillators in the inner coordination sphere.[41]

The metal-ion environments in the cavities of the imprinted polymers were probed by high-resolution luminescence of Eu^{III}.[42–44] The yttrium-free resins were treated in batch mode with aqueous solutions of europium chloride at pH 4 and analyzed by luminescence. The results were compared with those obtained for the parent complexes $[Eu(\mathbf{L1})_3]$ and $[Eu(\mathbf{L2})_3](ClO_4)_3$ (Figure 7, Table 5). At 77 K, the ligand-field splitting of the $[Eu(\mathbf{L1})_3]$ levels can be interpreted in terms of D_2 symmetry around the Eu^{III} ion.[42] The $^5D_0\rightarrow{}^7F_0$ transition is not detected, consistent with the fact that it is symmetry-forbidden in this point group. There are three main transitions to the $^7F_1$ level almost equally spaced ($\Delta E = 92$ and 74 cm^{-1}), corresponding to $A\rightarrow B_1$, B_2, B_3 transitions allowed in D_2 symmetry. The $^5D_0\rightarrow{}^7F_2$ transition displays two main components and a smaller (possibly split) one on the low-energy side consistent with the three allowed transitions in D_2; in addition, a very faint, vibronic component appears at 16 119 cm^{-1}. Finally, the $^5D_0\rightarrow{}^7F_4$ transition displays seven components, while six are predicted theoretically ($A\rightarrow 2B_1$, $2B_2$, $2B_3$). The emission spectrum of **R-Eu-L1** is very similar, both with respect to relative intensities and crystal-field splitting, that is, polymerization induces only minor changes in the Eu^{III} environment. It is noteworthy that the emission bands are not broadened, consistent with a homogeneous distribution of the sites.

The luminescence spectrum of $[Eu(\mathbf{L2})_3](ClO_4)_3$ is much simpler, with essentially one main component for $^5D_0\rightarrow{}^7F_1$

Table 5. Intensities of the $^5D_0\rightarrow{}^7F_J$ transitions relative to the magnetic dipole $^5D_0\rightarrow{}^7F_1$ transition, measured at 77 K on solid-state samples, and identified crystal-field sublevels [cm^{-1}] of the ^7F_J manifold ($^7F_0$ is taken as the origin); $\tilde{\nu}_{exc} = 36\,630$ cm^{-1}; v = vibronic.

Compound	$^7F_0$	$^7F_1$	$^7F_2$	$^7F_3$	$^7F_4$
			relative intensities		
$[Eu(\mathbf{L1})_3]$	0.01	1	1.34	0.01	0.27
R-Eu-L1	0.01	1	1.47	0.01	0.28
$[Eu(\mathbf{L2})_3]^{3+}$	0	1	2.48	0	0.30
R-Eu-L2	0.003	1	1.96	0.001	0.36
			crystal-field sublevels		
$[Eu(\mathbf{L1})_3]$	0	304, 396, 470	968, 1010, 1110, 1146(v)	1852, 1913	2679, 2730, 2810, 2856, 2897, 2967
R-Eu-L1	0	310, 396, 452	967, 1015, 1114, 1151, 1386	1851, 1912	2669, 2665, 2720, 2829, 2866, 2957, 3050
$[Eu(\mathbf{L2})_3]^{3+}$	0	384	994, 1099, 1140(v)	–	2677, 2833, 2850, 3050
R-Eu-L2	0	310, 384, 537	972, 1004, 1125	1832	2669, 2716, 2821, 2850, 3038

(possibly containing two closely spaced bands separated by 11 cm^{-1}), one intense and one small component for $^5D_0 \rightarrow {}^7F_2$ and three components for $^5D_0 \rightarrow {}^7F_4$. The $^5D_0 \rightarrow {}^7F_0$ and $^5D_0 \rightarrow {}^7F_3$ transitions are not observed. This is in line with the D_3 symmetry of the coordination polyhedron evidenced in the crystal structure (0, 2, 2 and 3 transitions are allowed for $J=$ 1, 1, 2, and 4, respectively[42]). On the other hand, the emission spectrum of the imprinted polymer **R-Y-L2** is quite different, with broad and split bands (three components for the $^5D_0 \rightarrow {}^7F_1$ transition, typical of low symmetry); this implies that polymerization results in severe distortion of the complexes and in an inhomogeneous distribution of the imprinted sites. The low emission intensity indicates that few europium cations are present in the resin.

Luminescence data therefore show that the imprinting of polymers with [Y(**L1**)$_3$] provides a resin with cavities retaining the appropriate coordination geometry. Good extraction and selectivity properties can then be expected for this resin, due to the template effect provided by the vicinity of three $\mathbf{L1}^-$ ligands in a geometry suitable for nonacoordination of any cation with an ionic radius close to that of yttrium. On the contrary, large changes in coordination environment occur in the case of the resin imprinted with [Y(**L2**)$_3$]-$(ClO_4)_3$ and fewer imprinted sites are available.

Yttrium extraction: Distribution coefficients were determined in batch mode with 500 mg of resin (170–230 mesh) at pH 4 in H_2O/EtOH 95:5 [Eq. (6)].

$$D = \left[\frac{c_i - c_f}{c_f}\right]\frac{V}{m} \qquad (6)$$

where c_i is the initial concentration of the cation, c_f the final concentration after equilibrium is reached, V the volume of the solution and m the quantity of resin. The distribution coefficient of **R-Y-L1** relative to yttrium is 570 $mL\,g^{-1}$, which is significantly larger than that of resin **R-L1** ($D=$ 35 $mL\,g^{-1}$), and the template effect is characterized by a D(**R-Y-L1**)/D(**R-L1**) ratio of 16. The "blank" polymer (resin **R**), resin **R-L2** and resin **R-Y-L2** do not extract any yttrium under the given experimental conditions ($D=$ 0 $mL\,g^{-1}$). Slight extraction of yttrium by **R-L1** is probably due to the presence of carboxyl groups in the resin, while **R-L2** is devoid of such groups. The lack of extraction of yttrium by **R-Y-L2** may be explained by the presence of perchlorate anions during the imprinting process of the resin, which are further removed upon acid washing.

Batch experiments were also carried out to determine the capacity of resin **R-Y-L1** to retain yttrium cations. Three runs involving 1 g of the resin and 20 mg of yttrium yielded a capacity of 8.9 ± 0.2 $mg\,g^{-1}$. Thus, the resin is able to extract macroquantities of yttrium when the pH is kept above 2.5. An estimate based on the quantities introduced in the synthetic procedure and on the quantity of extracted yttrium, leads to 44% of the complexation sites being active, which means that the porosity induced by DMSO and the hydrophilicity induced by allyl alcohol are optimum. In column experiments designed to determine the best extraction pH of the resin, 100% of the extraction capacity of the resin is achieved at pH 3.0. At pH 2, 60% extraction is reached, while at pH 1.0, only 15% of the extraction capacity is obtained. Thus, extraction of yttrium cations can be achieved at an acidic pH very suitable to avoid precipitation of hydroxide species, while in many literature reports extractions were conducted at a pH above 6, which reduces the validity of the methods.[13,18,45–47] The acidic character of cations with high charge density (e.g., lanthanides or Y^{III}) competes effectively with protons for complexation to the carboxyl groups of the dipicolinic moieties at pH <3.0. Rapid extraction kinetics are required due to the high elution rate used in column extraction chromatography. Two batch experiments carried out with 1 g of resin showed that the extraction kinetics are indeed very fast: 100% of the yttrium capacity is reached after only 10 min of contact of the resin with the spiked solution (10 mg Y, 50 mL, $t_{1/2}=1.7$ min, Figure 8a). Say et al. obtained an equilibrium time of 60 min in the extraction of copper(II) ions with an imprinted meth-

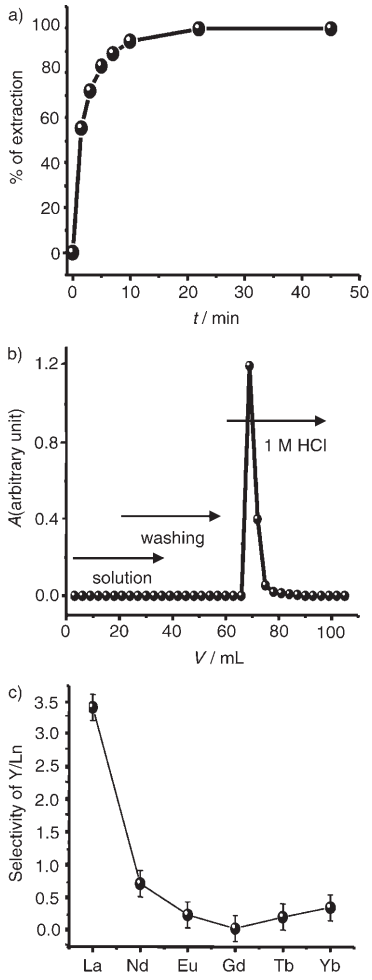

Figure 8. a) Extraction of 20 mg of Y^{III} by 0.5 g of **R-Y-L1** resin vs time (pH 4, $V=50$ mL). b) Elution profile of Y^{III} on a column containing 1 g of **R-Y-L1**. c) Selectivity of **R-Y-L1** along the lanthanide series (0.5 g **R-Y-L1**, 170–230 mesh, 10:10 mg Y:Ln, $V=50$ mL, pH 4, $t=20$ min).

acrylate polymer[3] and Biju et al. demonstrated that they could extract 100% of dysprosium from an aqueous solution at pH 6 in less than 5 min with an imprinted polystyrene polymer.[48] For extraction of Y^{III} or Ln^{III} ions from environmental samples or for production of medical radioactive sources, for example, ^{90}Y, elution profiles must show complete extraction of the metal ion, followed by a total elution from the column with a very small volume of the eluent solution. Figure 8b displays the results obtained for chromatographic experiments carried out on 2 g of **R-Y-L1**, starting with 20 mL of solution at pH 4, spiked with 10 mg of yttrium. The flow rate was 1 mL min^{-1} and the collected fractions amounted to 3 mL. Extraction of yttrium is clearly quantitative and the elution volume can be kept very small by using dilute hydrochloric acid: no significant change in the elution profile was noted when 1 M, 0.1 M or 0.05 M aqueous HCl was used to elute Y^{III} from the column. Such dilute media are of interest in view of medical radiolabelling applications. To test whether the resin can be used for preparation of medical-grade ^{90}Y, for example, without strontium and zirconium, the elution profile of a solution containing carrier-free ^{85}Sr, ^{88}Y and ^{95}Zr was determined (Figure 9):

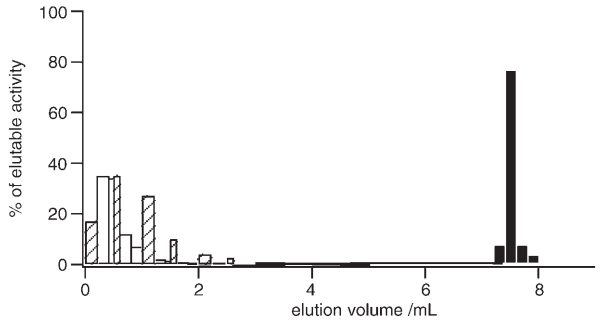

Figure 9. Elution profile of the radiotracer experiment on 200 mg of **R-Y-L1** resin. Black bars: ^{88}Y, hatched bars: ^{95}Zr, white bars: ^{85}Sr (from 0 to 7 mL: 0.001 M HCl, from 7 to 9 mL: 1 M HCl).

data show complete elution of ^{95}Zr and ^{85}Sr in a small volume of the loading solution, while ^{90}Y is completely retained on the column. The latter was subsequently eluted with less than 1 mL of 1 M HCl. Thus resin **R-Y-L1** could be of a great help to prepare very pure ^{90}Y from a long-period ^{90}Sr source with a minimum of handling, a challenging task in a nuclear medicine laboratory.

Selectivity of resin R-Y-L1: Resin **R-Y-L1** contains cavities matching the size of Y^{III}, which has an ionic radius close to those of the heavier Ln^{III} ions. In several batch experiments, pairs of Y/Ln cations were extracted by 500 mg of resin at pH 4.0. Distribution coefficients and selectivity were calculated by using Equations (6) and (7), respectively.

$$S_{Y/Ln} = D_Y/D_{Ln} \quad (7)$$

where D_Y is the distribution coefficient of yttrium, and D_{Ln} the distribution coefficient of the lanthanide ion. Selectivity for the heavier lanthanides (Figure 8c) is demonstrated by the larger S values for the lighter La^{III} and Nd^{III} ions. Selectivity was also tested in an experiment on a chromatographic column (2 g of **R-Y-L1**). Pairs of Y/Ln ions were extracted from 20 mL of solution at pH 4, and the selectivity was calculated as the ratio of the percentage of extracted Y^{III} to the percentage of extracted lanthanide. The obtained S' values range from 6 for Y/La to 0.5 for Y/Yb, and the selectivity sequence is La < Nd < Eu, Gd, Tb, Yb. Furthermore, the ion-imprinting effect, as measured by the increase in capacity when comparing **R-Y-L1** with blank **R-L1**, is large: a ratio of up to 16 was obtained. For comparison, Vignau et al. obtained a value smaller than 2 for Gd/La in the case of a resin imprinted with a 1:1 complex.[16] This could indicate that the increase in selectivity displayed by the latter resin is primarily driven by affinity, while in our case it is due to a size effect.

Finally, selectivity of **R-Y-L1** for Y^{III} over Ca^{II} and Sr^{II} was tested by batch extraction. For 0.5 g of resin, $D = 0$ mL g^{-1} for both alkaline earth metal ions. Additionally, two 10 mg samples of Y^{III} were extracted from 5 g samples of milk ash in 200 mL water on 2 g of **R-Y-L1**: Y^{III} recovery amounted to 72 ± 4%. Since milk ash contains large amounts of potassium, calcium and magnesium, this demonstrates that the resin is able to extract very small quantities (milligrams) of yttrium from macroquantities (grams) of alkali and alkaline earth metals. A much larger amount of resin is needed for a similar separation with a resin such as Dowex AG50w, for which the stability constant of the resin-metal complex plays a major role in the separation process. Moreover selective complexing agents such as ethylenediaminetetraacetic acid (EDTA) and α-hydroxyisobutyric acid (α-HIBA) are often necessary to improve the separation factor.[49,50] Thus ion-imprinted polymers with predefined cavities allowing size exclusion can improve the separation of metal cations. In this context, Rao et al. were able to separate Er^{III} from Y^{III}, Dy^{III}, Tb^{III} and Ho^{III} by solid-phase extraction using ion-imprinted polymer particles.[51]

Conclusion

We have demonstrated that imprinting a polymer with neutral [Y(**L1**)$_3$] complex, followed by acid demetallation, leads to a resin with high selectivity for Y^{III} and heavy Ln^{III} ions over calcium, strontium and potassium. Size exclusion of the lighter lanthanides from the preorganized cavity is thought to be the mechanism responsible for the observed selectivity, since neither calcium nor strontium was extracted by the imprinted resin in blank experiments with these ions. The obtained ion-imprinting effect stems from the rigid geometry imposed by the three dipicolinate-based ligand strands, which is maintained upon polymerization. The larger lanthanide cations such as La^{III} and Nd^{III} are prevented from entering the cavity tailored for Y^{III}, while the size mismatch is minimal for the heavier Ln^{III} ions. Overall, the reported

data open the way for the use of such resins for the production of medical-grade ^{90}Y, which necessitates a very high ^{90}Sr decontamination factor, as well as for the analysis of the highly toxic radiostrontium ^{90}Sr in milk and other foods by measurement of its daughter product ^{90}Y. The production of medical-grade radiolanthanides could also benefit greatly from this size-exclusion, imprinted-polymer technique. Further examples of radiotracer experiments and detailed analytical data obtained with the ion-imprinted resin based on $[Y(\mathbf{L1})_3]$ will be published elsewhere.[52]

Experimental Section

Materials and general methods: Analytical-grade chemicals were obtained from Merck, Acros, Fluka or Carlo-Erba. Divinylbenzene (Fluka) consisted of a 50:50% mixture of isomers. Ultrapure water was obtained with an SG Ultra-Clear UV apparatus. Reactions were conducted under inert atmosphere with standard Schlenk and dry-box techniques. THF was distilled from Na and benzophenone, and acetonitrile from CaH_2. Stock solutions of $Ln(ClO_4)_3{\cdot}n\,H_2O$ ($n=2.5$–4; Ln = Y, Eu, Tb, La, Gd) were prepared from lanthanide oxides[53] (99.99%, Rhône Poulenc) and the corresponding acid; concentrations were determined by complexometric titrations.[54] Elemental analyses were performed by Dr. Eder, Microchemical Laboratory of the University of Geneva.

Caution! Perchlorate salts of complexes with organic ligands are potentially explosive and should be handled in small quantities and with adequate precautions.[55]

^1H NMR and ^{13}C NMR spectra were recorded on a Bruker Avance DRX 400 spectrometer at 25 °C. Chemical shifts are given in ppm versus TMS. Positive-mode ES-MS spectra of 10^{-5}–10^{-4} M samples in CH_3CN or MeOH/H_2O were obtained with a Finningan SSQ 710C spectrometer calibrated with horse myoglobin (capillary temperature 200 °C, acceleration potential 4.5 kV, ion spray voltage 4.6 kV).

Photophysical measurements: UV/Vis absorption spectra were measured on a Perkin-Elmer Lambda 900 spectrometer using quartz Suprasil cells of 0.2 and 1 cm path length. Spectrophotometric titrations were performed with a J&M diode-array spectrometer (Tidas series) connected to a PC. Experiments were performed in a thermostated (25.0 ± 0.1 °C) glass-jacketed vessel at $\mu = 0.1$ M (KCl(aq) for **HL1**, and Et_4NCl in acetonitrile for **L2**). In a typical ligand titration, 50 mL of **L** was titrated with freshly prepared NaOH solutions at different concentrations (4, 1, 0.1 and 0.01 M). After each addition of base, the pH of the solution was measured by a KCl-saturated electrode, and UV/Vis absorption spectra were recorded with a Hellma optrode (optical path length 0.1 cm) immersed in the thermostated titration vessel and connected to the spectrometer. Factor analysis[56] and mathematical treatment of the data were performed with the SPECFIT program.[57,58]

Low-resolution luminescence measurements were recorded on a Fluorolog FL3-22 spectrometer from Horiba-Jobin-Yvon-Spex. Emission and excitation spectra were measured in 1 cm quartz Suprasil cells at room temperature (25 ± 0.1 °C, FL-1027 thermostated cell holder) and corrected for the instrumental function. Phosphorescence lifetimes were measured with the instrument in time-resolved mode, on frozen glycerol/water (10/90) or acetonitrile solutions at 77 K in a quartz capillary or a 1 cm Suprasil cell. They are averages of at least three independent measurements performed by monitoring the decay at the maxima of the emission spectra and enforcing a 0.03–0.05 ms time delay. All the decays were monoexponential and were analyzed using Origin 7.0.

X-ray crystallography: Single crystals suitable for X-ray diffraction were obtained by slow evaporation of a 10^{-3} M solution of **L1** in methanol and by diffusion of *tert*-butyl methyl ether into a 10^{-3} M solution of $[Eu(\mathbf{L2})_3](ClO_4)_3$ in MeCN. Data were not corrected for absorption. Structure solution and refinement as well as molecular graphics and geometrical calculations were performed with the SHELXTL software package, release 5.1.[59] Structures were refined by full-matrix least-squares techniques on F^2 with all non-H atoms anisotropically defined. H atoms were placed in calculated positions using the riding model. In the case of $[Eu(\mathbf{L2})_3](ClO_4)_3$, the disorder exhibited by two perchlorate anions and the solvent was treated by means of the split model and applying geometrical restraints. Data are reported in Table 6.

Table 6. Crystal data and structure refinement for **HL1** and $[Eu(\mathbf{L2})_3](ClO_4)_3$.

	HL1	$[Eu(\mathbf{L2})_3](ClO_4)_3{\cdot}2\,CH_3CN$
empirical formula	$C_{15}H_{12}N_2O_3$	$C_{73}H_{63}Cl_3EuN_{11}O_{18}$
formula weight	268.27	1640.65
crystal system	triclinic	triclinic
space group	$P\bar{1}$	$P\bar{1}$
a [Å]	8.458(2)	14.699(3)
b [Å]	8.656(3)	15.117(4)
c [Å]	8.750(2)	20.008(7)
α [°]	81.36(3)	83.54(3)
β [°]	87.53(2)	83.27(3)
γ [°]	79.15(3)	61.77(3)
V [Å^3]	621.9(3)	3881.7(18)
Z	2	2
$F(000)$	280	1672
μ [mm^{-1}]	0.102	0.985
T [K]	140(2)	140(2)
λ [Å]	0.71070	0.71070
reflns collected	3793	23525
ρ_{calcd} [Mg m^{-3}]	1.432	1.404
crystal size [mm^3]	0.09 × 0.09 × 0.08	0.20 × 0.15 × 0.15
θ range for data collection [°]	3.43–25.03	3.28–25.03
index ranges		
	$-10 \le h \le 10$	$-17 \le h \le 17$
	$-10 \le k \le 10$	$-17 \le k \le 17$
	$-10 \le l \le 10$	$-23 \le l \le 23$
independent reflections	2073	12811
R(int)	0.0363	0.0715
completeness to $\theta = 25.03$° [%]	94.0	93.6
data/restraints/parameters	2073/0/182	12811/390/1046
GOF on F^2	1.221	0.931
fnal R indices [$I > 2\sigma(I)$]		
R_1	0.0629	0.0974
wR_2	0.1473	0.2530
R indices (all data)		
R_1	0.0669	0.1577
wR_2	0.1558	0.3035
extinction coefficient	1.05(6)	0.0090(12)
largest diff. peak/hole [e Å^{-3}]	0.428/−0.510	1.614/−1.486

CCDC-286910 and -286911 contain the supplementary crystallographic data for this paper. These data can be obtained free of charge from the Cambridge Crystallographic Data Centre via www.ccdc.cam.ac.uk/data_request/cif.

Synthesis of the ligands (Scheme 1): Pyridine-2,6-dicarboxylic acid diethyl ester (**1**) and pyridine-2,6-dicarboxylic acid dimethyl ester (**2**) were synthesized according to Crystal et al.[31]

6-(4-Vinylphenylcarbamoyl)pyridine-2-carboxylic acid ethyl ester (3): Vinylphenylamine (95%, 5 g, 44 mmol) was dissolved in anhydrous THF (500 mL) under N_2. To this stirred solution, *n*-butyllithium (1.6 M in pentane, 27.5 mL, 44 mmol) was slowly added at RT. The yellow solution was stirred for 30 min and then added dropwise to a solution of **1** (10 g, 44.8 mmol) in THF (150 mL). The orange-brown solution was stirred overnight under N_2, and the solvents were removed by evaporation. The

brown residue was dissolved in CH_2Cl_2 (300 mL) and washed with water (2×300 mL), the organic layer dried over Na_2SO_4 and the solvent removed. The crude product was dissolved in diethyl ether (250 mL), yielding **L2** as precipitate (1 g, 8%). After evaporation of the filtrate, **3** was obtained as a pale yellow solid (10 g, 75%). ^{1}H NMR (400 MHz, $CDCl_3$): δ=10.09 (br, 1H, NH), 8.26 (d, J=7.8 Hz, 1H), 8.06 (d, J=7.7 Hz, 1H), 7.89 (dd, J=7.8, 7.7 Hz, 1H), 7.45 (d, J=8.6 Hz, 2H), 7.26 (d, J=8.6 Hz, 2H), 6.63 (dd, J=17.7, 10.9 Hz, 1H), 5.72 (d, J=17.7 Hz, 1H), 5.26 (d, J=10.9 Hz, 1H), 4.52 (q, 2H, OCH_2), 1.49 (t, 3H, CH_3); elemental analysis (%) calcd for $C_{17}H_{16}N_2O_3\cdot1.25\,H_2O$: C 64.04, H 5.85, N 8.79; found: C 64.09, H 5.77, N 8.67; ESI-MS: *m*/*z*: calcd for: 297.12; found: 297.58 $[M+H]^+$.

6-(4-Vinylphenylcarbamoyl)pyridine-2-carboxylic acid methyl ester (4): This compound was obtained in 72% yield by the procedure described for **3**, starting from diester **2**. ^{1}H NMR (400 MHz, $CDCl_3$): δ=10.07 (br, 2H, NH), 8.41 (d, J=7.8 Hz, 1H), 8.19 (d, J=7.7 Hz, 1H), 7.99 (dd, J=7.8, 7.7 Hz, 1H), 7.72 (d, J=8.6 Hz, 2H), 7.35 (d, J=8.6 Hz, 2H), 6.63 (dd, J=17.7, 10.9 Hz, 1H), 5.62 (d, J=17.7 Hz, 1H), 5.13 (d, J=10.9 Hz, 1H), 3.97 (s, 3H, OMe); ^{13}C NMR (400 MHz, [D$_6$]DMSO): δ=165.2, 161.49, 150.5, 146.7, 134.31, 137.4, 139.2, 127.8, 125.9, 127.2, 120.4, 136.5, 113.53, 53.43; elemental analysis (%) calcd for $C_{16}H_{14}N_2O_3\cdot0.25\,H_2O$: C 67.01, H 5.10, N 9.77; found: C 67.08, H 5.03, N 9.68; ESI-MS: *m*/*z*: calcd for: 283.10; found 283.30 $[M+H]^+$.

6-(4-Vinylphenylcarbamoyl)pyridine-2-carboxylic acid (HL1): A suspension of monoethyl ester **3** (10 g, 37.1 mmol) or monomethyl ester **4** (9.5 g, 31.7 mmol) in EtOH (80 mL) was gently refluxed until complete dissolution, then left to cool to RT before addition of 0.2 M NaOH (200 mL). The solution was stirred for 10 min at RT, EtOH was removed under vacuum at T<40 °C and water was added (300 mL). The aqueous phase was washed twice with CH_2Cl_2 (150 mL) and acidified to pH 2–3. The pale yellow precipitate was extracted with CH_2Cl_2 (3×200 mL). The organic layer was dried over Na_2SO_4, the solvent removed and **HL1** crystallized from hot MeCN to give a pale brown solid (8.5 g, 95%). M.p. 166–168 °C; ^{1}H NMR (400 MHz, [D$_6$]DMSO): δ=8.38 (d, J=7.3 Hz, 1H), 8.31 (d, J=7.6 Hz, 1H), 8.27 (dd, J=7.3, 7.6 Hz, 1H), 7.81 (d, J=8.5 Hz, 2H), 7.52 (d, J=8.5 Hz, 2H), 6.71 (dd, J=17.7, 11 Hz, 1H), 5.79 (d, J=17.7 Hz, 1H), 5.22 (d, J=11 Hz, 1H); ^{13}C NMR (400 MHz, [D$_6$]DMSO): δ=165.66, 162.3, 150.1, 147.05, 141.2, 138.6, 137.0, 134.2, 128.0, 127.6, 126.8, 121.5, 114.4; elemental analysis (%) calcd for $C_{15}H_{12}N_2O_3$: C 67.16, H 4.51, N 10.44; found: C 67.04, H 4.48, N 10.52; ESI-MS: *m*/*z*: calcd for: 269.08; found: 269.86 $[M+H]^+$.

Pyridine-2,6-dicarboxylic acid bis[(4-vinylphenyl)amide] (L2): *n*-Butyllithium (1.6 M in pentane, 11.8 mL, 18.7 mmol) was slowly added to vinylphenylamine (95%, 2.35 g, 18.7 mmol) in anhydrous THF (100 mL) with stirring at RT. The yellow solution was stirred for a further 30 min and then added dropwise to a solution of **2** (1.75 g, 9 mmol) in THF (150 mL). The orange-brown solution was stirred overnight under N_2 and the solvents were removed. The brown residue was dissolved in CH_2Cl_2 (200 mL) and washed with water (3×200 mL). The organic layer was dried over Na_2SO_4 and the solvent evaporated. The crude product was triturated in diethyl ether (150 mL), and the resulting solid was collected by filtration and dissolved in a minimum of CH_2Cl_2. Adding diethyl ether gave **L2** as a white solid, which was dried (2.8 g, 83%). (The filtrate contains mainly 6-(4-vinylphenylcarbamoyl)pyridine-2-carboxylic acid methyl ester (12% after purification) which can be treated as described for **3** and hydrolyzed to give **HL1**). M.p. >410 °C; ^{1}H NMR (400 MHz, $CDCl_3$): δ=9.52 (br, 2H, NH), 8.48 (d, J=7.9 Hz, 2H), 8.14 (dd, J=7.9, 8.5 Hz, 1H), 7.74 (d, J=8.5 Hz, 4H), 7.46 (d, J=8.5 Hz, 4H), 6.71 (dd, J=17.6, 10.8 Hz, 2H), 5.74 (d, J=17.6 Hz, 2H), 5.25 (d, J=10.8 Hz, 2H); ^{13}C NMR (400 MHz, $CDCl_3$): δ=161.4, 149, 4, 140.0, 137.0, 136.4, 134.9, 127.5, 126.0, 120.5, 113.9; elemental analysis (%) calcd for $C_{23}H_{19}N_3O_2$: C 74.78, H 5.18, N 11.37; found: C 74.27, H 5.07, N 11.29; ESI-MS: *m*/*z*: calcd for: 370.15; found: 370.78 $[M+H]^+$.

Synthesis of [Y(L1)$_3$]: NaOH (175 mg) in MeOH (20 mL, 4.01 mmol) was added to a solution of **HL1** (1 g, 3.7 mmol) in MeOH (100 mL) and the solution was stirred for 30 min at RT. A solution of $Y(ClO_4)_3\cdot2.8\,H_2O$ (544 mg, 1.2 mmol) in MeOH (50 mL) was added dropwise with vigorous stirring and a yellow precipitate formed. After stirring for a further 1 h, the solution was concentrated to half-volume, diethyl ether (150 mL) was added and the solid was separated by filtration, rinsed with cold MeOH and dried to give [Y(**L1**)$_3$] (1 g, 90%). ^{1}H NMR (400 MHz, [D$_6$]DMSO): δ=8.40 (d, J=6.9 Hz, 1H), 8.38 (d, J=8.5 Hz, 1H), 8.30 (dd, J=6.9, 8.5 Hz, 1H), 7.93 (d, J=8.6 Hz, 2H), 7.56 (d, J=8.6 Hz, 2H), 6.73 (dd, J=17.7, 10.7 Hz, 1H), 5.80 (d, J=17.7 Hz, 1H), 5.23 (d, J=10.7 Hz, 1H); ^{13}C NMR (400 MHz, [D$_6$]DMSO): δ=162.0, 149.2, 140.4, 138.1, 136.5, 133.6, 127.0, 125.7, 121.3, 113.8; elemental analysis (%) calcd for $C_{45}H_{33}N_6O_9Y$: C 60.68, H 3.73, N 9.44; found: C 60.79, H 4.31, N 9.11.

Synthesis of [Y(L2)$_3$](ClO$_4$)$_3$: **L2** (5 g 4 mmol) was dissolved in 50 mL of hot and dry MeCN and this solution was added dropwise at RT under vigorous stirring to a solution of $Y(ClO_4)_3\cdot2.8\,H_2O$ (585 mg, 1.3 mmol) in MeCN (50 mL). The solution turned yellow and a precipitate formed. After stirring for a further 1 h, the solution was concentrated to half its initial volume and the solid was collected by filtration, rinsed with cold MeCN and dried to give [Y(**L2**)$_3$](ClO$_4$)$_3$ (1 g, 89%). Elemental analysis (%) calcd for $C_{69}H_{57}Cl_3N_9O_{18}Y$: C 55.42, H 3.84, N 8.43; found: C 55.30, H 4.06, N 8.40.

Synthesis of [Ln(L1)$_3$] and [Ln(L2)$_3$](ClO$_4$)$_3$ (Ln=La, Eu, Gd, Tb): These complexes were synthesized according to the experimental procedures described above. Elemental analysis (%) calcd for $[La(\mathbf{L1})_3]\cdot1.25\,H_2O$: $C_{45}H_{33}N_6O_9La\cdot1.25\,H_2O$: C 56.11, H 3.71, N 8.73; found: C 56.13, H 3.91, N 8.36; elemental analysis (%) calcd for $[Eu(\mathbf{L1})_3]\cdot H_2O$: $C_{45}H_{33}N_6O_9Eu\cdot H_2O$: C 55.62, H 3.63, N 8.65; found: C 55.62, H 3.81, N 8.47; elemental analysis (%) calcd for $[Gd(\mathbf{L1})_3]\cdot0.7\,H_2O$: $C_{45}H_{33}N_6O_9Gd\cdot0.7\,H_2O$: C 55.63, H 3.57, N 8.65; found: C 55.62, H 4.38, N 8.53; elemental analysis (%) calcd for $[Tb(\mathbf{L1})_3]\cdot0.7\,H_2O$: $C_{45}H_{33}N_6O_9Tb\cdot0.7\,H_2O$: C 55.53, H 3.56, N 8.64; found: C 55.55, H 3.74, N 8.44; elemental analysis (%) calcd for $[La(\mathbf{L2})_3](ClO_4)_3\cdot2\,H_2O$: $C_{69}H_{57}Cl_3N_9O_{18}La\cdot2\,H_2O$: C 52.40, H 3.89, N 7.97; found: C 51.97, H 3.62, N 7.49; elemental analysis (%) calcd for $[Eu(\mathbf{L2})_3](ClO_4)_3\cdot0.5\,H_2O$: $C_{69}H_{57}Cl_3N_9O_{18}Eu\cdot0.5\,H_2O$: C 52.87, H 3.73, N 8.04; found: C 52.57, H 3.98, N 8.59; elemental analysis (%) calcd for $[Gd(\mathbf{L2})_3](ClO_4)_3\cdot3.7\,H_2O$: $C_{69}H_{57}Cl_3N_9O_{18}Gd\cdot3.7\,H_2O$: C 50.83, H 3.98, N 7.73; found: C 50.50, H 3.96, N 7.57; elemental analysis (%) calcd for $[Tb(\mathbf{L2})_3](ClO_4)_3\cdot2\,H_2O$: $C_{69}H_{57}Cl_3N_9O_{18}Tb\cdot2\,H_2O$: C 51.75, H 3.84, N 7.87; found: C 51.66, H 3.85, N 7.94.

Synthesis and characterization of the yttrium resins: Resin **R-Y-L1**: Complex [Y(**L1**)$_3$] (1 g, 1.12 mmol), DMSO (3 mL), divinylbenzene (3 mL), pyridine (3 mL), allyl alcohol (3 mL) and of azobis(isobutyronitrile) (25 mg) were introduced into a tube containing a magnetic stirrer. The tube was purged under vacuum and filled with argon. It was placed in an ultrasonic bath and sonicated for 15 min under argon to remove any trace of oxygen. Caution must be taken never to stop agitation when degassing the polymer mixture, otherwise a sticky precipitate appears which can only be redissolved with difficulty. The tube was then sealed and placed in an oil bath at 85 °C for 12 h. Polymerization was conducted with vigorous stirring to allow for good dispersion of the complex into the polymer. Finally, the tube was crushed; the crude product washed with methanol and then coarsely crushed in a mortar. The bulk product was washed successively in methanol, ethanol, and water/ethanol 90:10 several times. Finally, the product was washed with 5 M HCl to remove the yttrium template, then several times with water and allowed to dry. The yttrium-free resin **R-Y-L1** was finely ground in a mortar and the fractions 60–120 mesh, 120–170 mesh, 170–230 mesh and >230 mesh were separated with a set of minisieves.

The other resins were synthesized by using a slightly modified procedure: **R-Y-L2** was obtained from [Y(**L2**)$_3$](ClO$_4$)$_3$) (1 g, 0.67 mmol) and without DMSO; for resin **R**, no complex was added; for resin **R-L1**, **HL1** (900 mg, 3.26 mmol) was added instead of [Y(**L^1**)$_3$]; for resin **R-L2**, **L2** (740 mg, 2 mmol) was added instead of [Y(**L2**)$_3$](ClO$_4$)$_3$); for resin **R-Eu-dpa**, [Cs$_3$Eu(dpa)$_3$] (468 mg, 0.448 mmol) was added instead of [Y(**L1**)$_3$].

Analytical measurements: Chromatographic elution profiles and yttrium yield were determined by atomic absorption (410.2 nm) with a Perkin Elmer 4100 atomic spectrometer using a N_2O/acetylene flame. Calcium (422.7 nm) and strontium (460.7 nm) were determined in the same way using an air/acetylene flame. In the selectivity experiment Y, La, Nd, Eu, Gd, Tb and Yb were determined by atomic emission with a Perkin

Elmer ICP-AES spectrometer Optima 2000 DV. Multiple-wavelength analysis was used. Chromatographic columns were made of 2 g of the yttrium resin in a 6 mL Supelco column 57242. Supelco no. 57273-U column adaptor and Ismatec IPS-12 peristaltic pump were used to pump the solutions into the column.

Column preparation: The resin (2 g, 60–120 mesh) was dispersed in water containing 5% ethanol and stirred for 15 min before introducing the mixture into a 6 mL Supelco no. 57242 column; a Teflon frit was added on top of the resin bed. A Supelco no. 57273-U tube adapter was clamped to the column to allow utilization of the column with a peristaltic pump (Ismatec IPS-8), overpressure being necessary for the solution to pass through the column. Elution profiles were recorded with 20 mL of a solution containing 10 mg of yttrium at pH 4. Fractions of 3 mL were collected and yttrium content determined by atomic absorption.

Batch experiments: 0.5 g of resin (170–230 mesh) was suspended in water (50 mL) containing 5% ethanol and the pH was adjusted to 4. Y (10 mg), Ca (10 mg), Sr (10 mg) or Y/Ln pairs (10 mg/10 mg) were introduced as standard chloride solutions at pH 4. After equilibrium was reached (ca. 20 min), an aliquot of the supernatant (1 mL) was sampled and filtered (0.45 μm) in a syringe, and the Y or Ln content determined by atomic absorption or ICP-AES. Kinetic experiments were performed in the same way; aliquots of 1 mL were taken after 0.5, 1.5, 3, 5, 7, 10, 20 and 40 min. Errors in batch experiments were estimated to be 5%, mainly due to AA or ICP-AES determination and loss in filtration.

Radiotracer experiment: All experiments were performed with ^{85}Sr (94028 ± 990 Bq mL^{-1}, ^{95}Zr (148000 ± 376 Bq mL^{-1}) and ^{88}Y(74000 ± 2200 Bq mL^{-1}) standard solutions; 200 mg of the resin (>170 mesh) was suspended in water containing 5% ethanol and stirred for 15 min before introducing the mixture in a Fa. EiChrom column. 100 μL of each standard solution was pipetted, the mixture evaporated to dryness and redissolved in 1 mL of 0.001 M HCl, then poured onto the column. Elution was carried out with 0.001 M HCl, then with 1 M HCl. Fractions of 0.2 mL were collected. The ^{85}Sr and ^{88}Y activities were determined by liquid scintillation counting (LSC, Packard MINAXI TriCarb or LKB Wallac 1220) or by γ spectrometry (HPGe detectors). ^{95}Zr was determined by γ spectrometry.

Extraction of yttrium from milk samples: Milk ash (5 g) was dissolved in 32% HCl (20 mL) and YCl_3 was added (10 mg). The mixture was heated to allow slow evaporation of the acid. When the volume reached about 5 mL, water was added (200 mL). If necessary, the solution was filtered. 2.5 M NaOH was added to raise the pH as close as possible to 3.0 while avoiding precipitation of calcium phosphate. The solution was pumped into the column (2 g resin) at a rate of 1 mL min^{-1}. After washing the column with water (20 mL), Y^{III} was eluted with 1 M HCl (10 mL) and the yield was determined by atomic absorption spectrometry.

Acknowledgements

We thank Timothé Schmittler and Lucy Layaz for their technical help, Alexander Schiller for the ICP measurements and Dr. Daniel Imbert and Frédéric Gumy for their contribution to the luminescence measurements. This work is supported by the Swiss National Science Foundation, and the Swiss Federal Office of Public Health (contract No. 3189.001.4).

[1] G. M. Murray, G. E. Southard, *Molecularly Imprinted Materials* (Eds.: M. Yan, O. Ramstroem), Marcel Dekker, New York, **2005**, pp. 579–602.
[2] D. Atzei, T. Ferri, C. Sadun, P. Sangiorgio, R. Caminiti, *J. Am. Chem. Soc.* **2001**, *123*, 2552–2558.
[3] R. Say, E. Birlik, A. Ersöz, F. Yilmaz, T. Gedikbey, A. Denizli, *Anal. Chim. Acta* **2003**, *480*, 251–258.
[4] L. Wu, Y. Li, *Anal. Chim. Acta* **2003**, *482*, 175–181.
[5] S. Y. Bae, G. L. Southard, G. L. G. M. Murray, *Anal. Chim. Acta* **1999**, *397*, 173–181.
[6] G. Vlatakis, L. I. Andersson, R. Müller, K. Mosbach, *Nature* **1993**, *361*, 645–646.
[7] G. Wulff, *Angew. Chem.* **1995**, *107*, 1001–1002; *Angew. Chem. Int. Ed. Engl.* **1995**, *34*, 1812–1832.
[8] J.-Q. Liu, G. J. Wulff, *J. Am. Chem. Soc.* **2004**, *126*, 7452–7453.
[9] J. Svenson, N. Zheng, I. A. Nicholls, *J. Am. Chem. Soc.* **2004**, *126*, 8554–8560.
[10] M. Subat, A. S. Borovik, B. König, *J. Am. Chem. Soc.* **2004**, *126*, 3185–3190.
[11] H.-H. Yang, S.-Q. Zhang, F. Tan, Z.-X. Zhuang, X.-R. Wang, *J. Am. Chem. Soc.* **2005**, *127*, 1378–1379.
[12] S. M. D′Souza, C. Alexander, S. W. Carr, A. M. Waller, M. J. Whitcombe, E. N. Vulfson, *Nature* **1999**, *398*, 312–316.
[13] V. K. Jain, A. Handa, S. S. Sait, P. Shrivastav, Y. K. Agrawal, *Anal. Chim. Acta* **2001**, *429*, 237–246.
[14] T. Suzuki, M. Aida, Y. Ban, Y. Fujii, M. Hara, T. Mitsugashira, *J. Radioanal. Nucl. Chem.* **2003**, *255*, 581–583.
[15] H. C. Lo, H. Chen, R. H. Fish, *Eur. J. Inorg. Chem.* **2001**, 2217–2220.
[16] O. Vigneau, C. Pinel, M. Lemaire, *Anal. Chim. Acta* **2001**, *435*, 75–82.
[17] O. Güney, Y. Yilmaz, Ö. Pekcan, *Sensors Actuators B* **2002**, *85*, 86–89.
[18] L. S. Molochnikov, E. G. Kovalyova, A. A. Zagorodni, M. Muhammed, Y. M. Sultanov, A. A. Efendiev, *Polymer* **2003**, *44*, 4805–4815.
[19] C. T. Horovitz, *Biochemistry of Scandium and Yttrium*, Part 1, Kluwer Academic/Plenum Publishers, New York, **1999**.
[20] K. Okamoto, S. Fukuzumi, *J. Am. Chem. Soc.* **2004**, *126*, 13922–13923.
[21] S. Malja, K. Schomaker, E. Malja, *J. Radioanal. Nucl. Chem.* **2000**, *245*, 403–406.
[22] L. S. Park, L. P. Szajek, K. J. Wong, P. S. Plascjak, K. Garmestani, S. Googins, W. C. Eckelman, J. A. Carrasquillo, C. H. Paik, *Nucl. Med. Biol.* **2004**, *31*, 297–301.
[23] M. L. Dietz, E. P. Horwitz, *Appl. Radiat. Isot.* **1992**, *43*, 1093–1101.
[24] S. Liu, *Chem. Soc. Rev.* **2004**, *33*, 445–461.
[25] E. P. , Horwitz, R. Chiarizia, M. L. Dietz, H. Diamond, *Anal. Chim. Acta* **1993**, *281*, 361–372.
[26] E. P. Horwitz, M. L. Dietz, D. E. Fisher, *Anal. Chem.* **1991**, *63*, 522–525.
[27] F. Rösch, E. Forssell-Aronsson, *Metal Ions in Biological Systems* (Eds.: A. Sigel, H. Sigel), Marcel Dekker, New York, Basel, **2004**, Vol. 42, Chap. 3.
[28] E. P. Horwitz, R. Chairizia, M. L. Dietz, *Solvent Extr. Ion Exch.* **1992**, *10*, 313.
[29] P. Froidevaux, J.-J. Geering, J.-F. Valley, *J. Radioanal. Nucl. Chem.* **2002**, *254*, 23–27.
[30] P. Froidevaux, K. Friedrich-Bénet, J.-F. Valley, *J. Radioanal. Nucl. Chem.* **2004**, *261*, 295–299.
[31] E. J. T. Crystal, L. Couper, D. J. Robins, *Tetrahedron* **1995**, *51*, 37, 10241–10252.
[32] A.-S. Chauvin, R. Tripier, J.-C. G. Bünzli, *Tetrahedron Lett.* **2001**, *42*, 3089–3091.
[33] R. M. Tichane, W. E. Bennett, *J. Am. Chem. Soc.* **1957**, *79*, 1293–1296.
[34] D. C. Crans, L. Yang, T. Jakush, T. Kiss, *Inorg. chem.* **2000**, *39*, 4409–4416.
[35] F. Renaud, C. Piguet, G. Bernardinelli, J.-C. G. Bünzli, G. Hopfgartner, *Chem. Eur. J.* **1997**, *3*, 1646–1659.
[36] F. Renaud, C. Piguet, G. Bernardinelli, J.-C. G. Bünzli, G. Hopfgartner, *Chem. Eur. J.* **1997**, *3*, 1660–1667.
[37] P. A. Brayshaw, J.-C. G. Bünzli, P. Froidevaux, J. M. Harrowfield, Y. Kim, A. N. Sobolev, *Inorg. Chem.* **1995**, *34*, 2068–2076.
[38] I. Grenthe, *J. Am. Chem. Soc.* **1961**, *83*, 360–364.
[39] K. Nakamoto, *Infrared and Raman Spectra of Inorganic and Coordination Compounds*, Wiley-Interscience, New York, **1990**.
[40] L. Puntus, V. Zolin, V. Kudryashova, *J. Alloys Compd.* **2004**, *374*, 330.

[41] J.-C. G. Bünzli, P. Froidevaux, C. Piguet, *New J. Chem.* **1995**, *19*, 661–668.
[42] J.-C. G. Bünzli, in *Lanthanide Probes in Life, Chemical and Earth Sciences* (Eds.: J.-C. G. Bünzli, G. R. Choppin), Elsevier, Amsterdam, **1989**, Chap. 7.
[43] J.-C. G. Bünzli, C. Piguet in *Encyclopedia of Materials: Science and Technology, Vol. 10* (Eds.: K. H. J. Buschow, R. W. Cahn, M. C. Flemings, B. Ilschner, E. J. Kramer, S. Mahajan), Elsevier Science, Oxford, **2001**, Chapter 1.10.4, p. 4465ff.
[44] J.-C. G. Bünzli in *Spectroscopy of Rare Earths in Optical Materials* (Eds.: G. K. Liu, B.Jacquier), Springer, Berlin, **2005**, Chapter 11.
[45] R. Say, E. Birlik, A. Ersoz, F. Yilmaz, T. Gedikbey, A. Denizli, *Anal. Chim. Acta* **2003**, *480*, 251–258.
[46] A. Ersöz, R. Say, A. Denizli, *Anal. Chim. Acta* **2004**, *512*, 63–67.
[47] P. Metilda, J. Mary Gladis, T. Prasada Rao, *Anal. Chim. Acta* **2004**, *512*, 63–73.
[48] V. M. Biju, J. Mary Gladis, T. Prasada Rao, *Anal. Chim. Acta* **2003**, *478*, 43–51.
[49] J.-J. Geering, C. Friedli, P. Lerch, *J.Trace Microprobe Tech.* **1990**, *8*, 211–230.
[50] S. Lahiri, K. J. Volkers, B. Wierczinski, *Appl. Radiat. Isot.* **2004**, *61*, 1157–1161.
[51] R. Kala, J. M. Gladis, T. P. Rao, *Anal. Chim. Acta* **2004**, *518*, 143–150.
[52] P. Froidevaux, S. Happel, A.-S. Chauvin, *Chimia* **2006**, *60*, 203–206.
[53] J. F. Desreux in *Lanthanide Probes in Life, Chemical and Earth Sciences* (Eds.: J.-C. G. Bünzli, G. R. Choppin), Elsevier, Amsterdam, **1989**, Chapter 2, p. 43.
[54] G. Schwarzenbach, *Complexometric Titrations*, Chapman and Hall, London, **1957**.
[55] K. N. Raymond, *Chem. Eng. News* **1983**, *61*, 4–4.
[56] E. R. Malinowski, D. G. Howery, *Factor Analysis in Chemistry*, Wiley, New York, Chichester, **1980**.
[57] H. Gampp, M. Maeder, C. J. Meyer, A. D. Zuberbühler, *Talanta* **1985**, *32*, 1133–1139.
[58] H. Gampp, M. Maeder, C. J. Meyer, A. D. Zuberbühler, *Talanta* **1986**, *33*, 943–951.
[59] DELABS, N. Walker, D. Stuart, *Acta Crystallogr. Sect. A* **1983**, *39*, 158–166.

Received: November 3, 2005
Revised: March 1, 2006
Published online: June 8, 2006

